Journal of Molecular Liquids 294 (2019) 111655

Contents lists available at ScienceDirect

Journal of Molecular Liquids

journal homepage: www.elsevier.com/locate/molliq

Gold(III) complex from pyrimidine and morpholine analogue Schiff base ligand: Synthesis, characterization, DFT, TDDFT, catalytic, anticancer, molecular modeling with DNA and BSA and DNA binding studies

Murugesan Sankarganesh [a], Jeyaraj Dhaveethu Raja [b,*], Nagaraj Revathi [c], Rajadurai Vijay Solomon [d], Raju Senthil Kumar [e]

[a] Department of Chemistry, K. Ramakrishnan College of Technology, Samayapuram, Trichy, Tamil Nadu 621 112, India
[b] Department of Chemistry, The American College, Tallakkualm, Madurai, Tamil Nadu 625 002, India
[c] Department of Chemistry, Ramco Institute of Technology, Rajapalayam, Virudhunagar, Tamil Nadu 626 117, India
[d] Department of Chemistry, Madras Christian College (Autonomous), Tambaram East, Chennai 600 059, Tamil Nadu, India
[e] Department of Pharmaceutical Chemistry, Swami Vivekanandha College of Pharmacy, Elayampalayam, Trichengode, Namakkal, Tamil Nadu 637 005, India

ARTICLE INFO

Article history:
Received 26 June 2019
Received in revised form 24 August 2019
Accepted 27 August 2019
Available online 28 August 2019

Keywords:
Au(III) complex
Molecular modeling
DNA interaction
In vitro
in vivo anticancer studies

ABSTRACT

New gold(III) complex, $[AuL_2]Cl_3$ was synthesized from (2-(4-morpholinobenzylidene)-1-(4-(trifluoromethyl) pyrimidin-2-yl)hydrazine) and characterized by analytical and miscellaneous spectral methods. These results show that Au(III) complex has square planar geometry. Density functional theory (DFT) calculations have been done to understand the electronic structure of the Au(III) complexand free ligand while time dependent density functional theory (TDDFT) calculations have been employed to compute absorption spectra of ligand and Au(III) complex. Antimicrobial results suggest that ligand and complex have been inhibited the *E. coli* bacteria (13 mm) and *C. albicans* fungi (16 mm) than other microbes. Antioxidant results exhibit the ligand and complex has enhanced scavenging activities against several free radicals. *In vitro* anticancer activities of cisplatin, ligand and complex have been explored by MTT assay against various human cancer cell lines (breast-MCF-7, liver-HepG2, cervical-HeLa, lung-A549) and one normal cell line (NHDF- normal human dermal fibroblasts). The results show that complex has low IC_{50} values against cancer cell lines (20.6 ± 0.98 μg/mL, MCF-7; 22.68 ± 1.13 μg/mL, HepG2; 32.00 ± 1.60 μg/mL, HeLa; 33.19 ± 1.66 μg/mL, A549) than ligand. Moreover, complex has ten times least toxic activity (109.65 ± 5.48 μg/mL) on NHDF cell line as compared to cisplatin (10.28 ± 0.51 μg/mL). Based on the least toxic activity of complex has been further discovered by *in vivo* anticancer study using Ehrlich Ascites Carcinoma (EAC) tumor bearing Swiss albino mice. DNA interactions of ligand and complex have been studied by electronic absorption, fluorescence, viscometric and cyclic voltammetic methods. The results suggest that ligand and complex binds with CT-DNA through an intercalative interaction. Further confirm the nature of interaction between ligand and Au(III) complex towards DNA and BSA protein, molecular docking analysis has been carried out. These results reveal that Au(III) complex shows greater binding ability towards DNA and BSA than the ligand.

1. Introduction

In the sixteenth century, transition metal complexes have been used in the treatment of cancer and leukemia. In 1960, the antitumor activity of platinum metal based complex of cisplatin was introduced [1]. The platinum based drugs like carboplatin, oxaliplatin, nedaplatin and iproplatin have been utilized in the cancers treatment. The successive results obtained from platinum metal based complexes are encouraged to develop the antitumor drugs from other transition metal complexes [2–5]. Among the transition metal complexes, the gold(III) metal complexes are significant role in the biological and pharmacological studies. Interestingly, auranofin is a familiar gold metal based antiarthiritic drug has been utilized as anticancer agent against most of the cancers [6–8]. Hence, the investigations on anticancer activity of gold metal complexes have intense attention in recent decades.

Many literature reports of biological studies have established that DNA is the major intracellular target of a number of antitumor drugs [9]. In the molecular biology, DNA act as a genetic information carrier which often targets for metal based drugs. These metal based drugs can affect the DNA replication, cell growth, cell division, transcription and protein synthesis [10]. Moreover, the interaction of DNA with transition metal complexes is considerable interest in the designing new DNA-targeted metal based drugs [11,12].

* Corresponding author.
E-mail address: jdrajapriya@gmail.com (J.D. Raja).

https://doi.org/10.1016/j.molliq.2019.111655
0167-7322/

In living cell metabolism, nitrogen-containing heterocycles and pyrimidine derivatives are exclusively playing a very important role. It is prevalent in nature and is necessary for human life [13]. It's like that, the morpholine derivatives are widely used antibiotic agents like, Linezolid [14]. A great compact of awareness has been contributed to the synthesis of Schiff base ligand containing pyrimidine and morpholine backbones.

Molecular docking analysis is known to shed light on the binding preferences of metal complexes towards DNA and proteins in general and offers the information about the stabilizing interactions inside the active site in particular [15,16].

In this research report, a new Au(III) complex was prepared from pyrimidine and morpholine derivative Schiff base and characterized by various spectroscopic and analytical methods. Furthermore, various biological applications (antimicrobial, antioxidant, DNA interaction, BSA interaction and anticancer (*in vitro* and *in vivo*)) were studied. In order to get the correct conformation of the metal complex and the free ligand, density functional theory (DFT) calculations have been performed. The optimized geometries from DFT calculations are considered for molecular docking analysis. Further, time dependent density functional theory (TDDFT) calculations have been carried out to estimate the absorption spectra of metal complex and free ligand. The results are compared with experimental results.

2. Experimental protocols

2.1. Materials and instrumentation

4-(4-morpholinyl)benzaldehyde, 2-hydrazino-4-(trifluoromethyl) pyrimidine, $HAuCl_4.3H_2O$, Tris-HCl, sodium chloride and ethidium bromide were procured from sigma aldrich company. Calf-thymus (CT) DNA was purchased from GENEI Bangalore, India. Elemental analyses were recorded on an Elementar Vario EL III analyzer. The absorption spectra and Fluorescence spectra were recorded on UV-1800 (Shimadzu) spectrophotometer and Fluoromax-4 spectrometer, respectively. FTIR spectra and ^1H NMR spectra were recorded on FTIR (IR affinity-1, Shimadzu) instrument and Bruker (400 MHz) spectrometer using $SiMe_4$ as the internal standard. The mass spectra were obtained by ESI-MS spectrometer and ESR spectra were recorded at 300 and 77 K in IIT, Mumbai using TCNE (tetracyanoethylene) as the g-marker. Electrochemical studies were demonstrated on a CHI650C instrument.

2.2. Synthesis of ligand

Ligand was synthesized from 4-(4-morpholinyl)benzaldehyde and 2-hydrazino-4-(trifluoromethyl)pyrimidine and reported in earlier literature [17].

2.3. Synthesis of Au(III) complex

The ligand (2 mmol) was dissolved in acetone (10 mL). To this solution, 10 mL ethanolic solution of metal chloride salt was added in dropwise. The resulting mixture was refluxed under stirring for 5 h. Then the solution was evaporated on a water bath, the precipitated solid was filtered and washed thoroughly with petroleum ether (10 mL) and dried *in vacuo*.

Au(III) complex: Yield (65%), Color: Dark brown, MP: 230 °C, ^1H NMR: δ 8.67 (s, 1H) 9.82 (s, 1H), 7.17 (d, 1H), 9.50 (d, 1H), 7.10 (d, 2H), 7.76 (d, 2H), 3.40 (t, 4H), 3.85 (t, 4H) ppm, IR (KBr disc): ν 1523 (CH=N), 1589 (bend, -NH), 3516 (stretch, -NH), 1463 and 1389 (aromatic, CF_3-CH=N- and C=N), 1315 (aromatic, C—N), 3051 and 3032 (aromatic *sym* and *asym*, C—H), 1150 (CF_3), 2937 and 2881 (aliphatic sym and asym, C—H), 1091 and 1230 (sym and asym, C-O-C), 1186 (morpholino-C-N) cm^{-1}; UV–visible (λ_{max}): 243, 324, 529 nm; ESI Mass: 896 (m/z); Anal. Cacld (%) for $C_{32}H_{32}N_{10}O_2F_6Au$: C, 42.7; H, 3.56; N, 15.57; Au, 21.91; Found (%): C, 42.1; H, 3.49; N, 15.49; Au, 21.85.

2.4. Antimicrobial activities

Antimicrobial activities of ligand and Au(III) complex were studied against *Escherichia coli (E. coli-2599), Klebsiella pneumonia (K. pneumonia-BAA2342), Pseudomonas fluorescens (P. fluorescens-17,400), Shigella sonnei (S. sonnei-9290) & Staphylococcus aureus (S. aureus-25,923)* and fungal species, *Aspergillus niger (A. niger-6275), Candida albicans (C. albicans-2091), Candida tropicalis (C. tropicalis-13,803), Mucor indicus (M. indicus-4857) & Rhizopus oligoporous (R. oligoporous-60,826)* by the well diffusion method. The standard drugs like streptomycin and amphotericin were used for antibacterial and antifungal studies.

2.5. In Vitro anticancer study

The *in vitro* anticancer activity of free ligand and Au(III) complex were studied against MCF-7, HeLa, HEp-2 and NHDF cell lines by using MTT [3-(4,5-dimethyl-2-thiazolyl)-2,5 diphenyl-2-H-tetrazolium bromide)] assay [18]. The percentage growth inhibition was calculated using the following formula,

$$\%growth\ inhibition = \frac{Mean\ OD\ of\ individual\ test\ group}{Mean\ OD\ of\ control\ group} \times 100$$

2.6. In vivo anticancer study

2.6.1. Animals used

Healthy Swiss albino mice weighing 20.0 ± 2.0 g was used for the antitumor studies. The animals were housed in polypropylene cages and maintained under standard conditions (25 ± 2 °C) with 12 h dark/light cycle. The animals were fed with standard animal pellet diet and water *ad libitum*. The study was conducted as per the CPCSEA guidelines and the study was approved by Institutional Animal Ethics Committee (IAEC) of Swamy Vivekananda College of Pharmacy, Tamil Nadu, India (880/ac/16/1317 dated 13.11.2015).

2.6.2. Acute toxicity studies

Acute oral toxicity study of Au(III) complex was examined by acute toxicity methods as per the organization for Economic Co-operation and Development (OECD) guidelines for testing of chemicals OECD, 423 (Acute Oral Toxicity-Acute Toxic class method) [19]. The detailed procedure is expressed in supplementary section (S1-S4).

2.7. DNA interaction

DNA interactions of ligand and Au(III) complex with CT-DNA were carried out by using electronic absorption & fluorescence spectral titrations, viscosity measurements and electrochemical investigations in appropriate buffer solutions [20,21].

2.8. Computational studies

B3LYP/LANL2DZ level of theory has been used to optimize the Au(III) complex while the free ligand is optimized using 6-31 g(d) basis set. Gaussian 09 software package is used for the DFT and TDDFT calculations. Autodock Vina software is used for the molecular docking calculations [22,23]. Optimized geometries are given in Fig. 1 while their HOMO and LUMOs are collected in Fig. 2. All real frequencies in the frequency analysis confirm that the obtained geometries are at their ground state. AUTODOCK Vina software is used for the molecular docking studies [23]. The DNA (PDB ID:355D) and BSA (PDB ID:4F5S) protein three dimensional structures are extracted from protein data

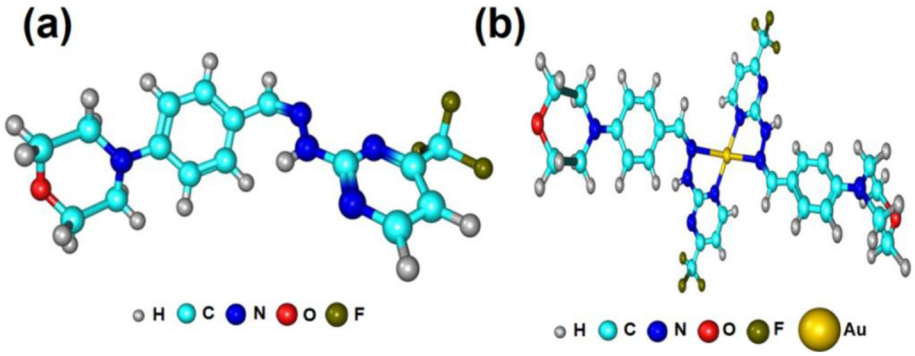

Fig. 1. DFT optimized geometry of ligand (a) and Au(III) complex (b).

bank (PDB) [24] Docking is processed with the setting of the grid sizes 60, 60 and 60 along the X-, Y- and Z-axes.

2.9. Catalytic reduction with $NaBH_4$

The reduction of *p*-nitrophenol (*p*-NP) to *p*-aminophenol (*p*-AP) by $NaBH_4$ using the Au(III) complex as a catalyst was studied [25]. In this experiment, 2.7 mL of p-NP (2×10^{-5}) was mixed with 0.2 mL of $NaBH_4$ (reducing agent). The electronic absorption of above blank solution was recorded in the range of 200–700 nm. Then, 0.1 mL solution of Au(III) complex (1 mmol) was added to the above mixture and recorded the absorption spectrum in the range of 200–700 nm at different time intervals (0–12 min).

3. Result and discussion

3.1. Chemistry

Ligand was synthesized from 4-(4-morpholinyl)benzaldehyde and 2-hydrazino-4-(trifluoromethyl)pyrimidine and reported in previously published literature [17]. Herein, we reported the synthesis of Au(III) complex from Schiff base ligand containing pyrimidine and morpholine analogues in ethanol under reflux condition (Scheme 1). The analytical, physicochemical and spectral data of ligand and Au(III) complexare recapitulated in experimental section.

Au(III) complex is dark brown color and soluble in ethanol, DMSO and DMF solvents. The results of mass and elemental analysis for the

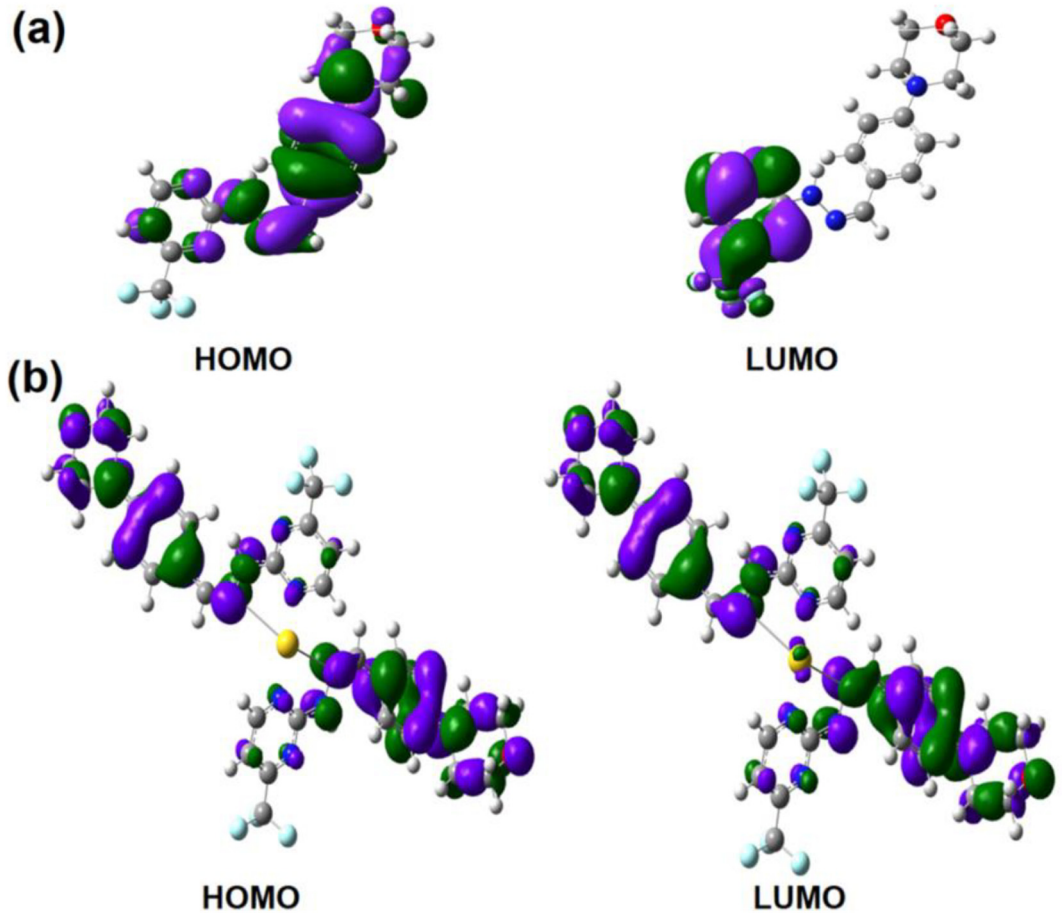

Fig. 2. HOMO and LUMO of free ligand (a) and Au(III) complex (b) from DFT calculations.

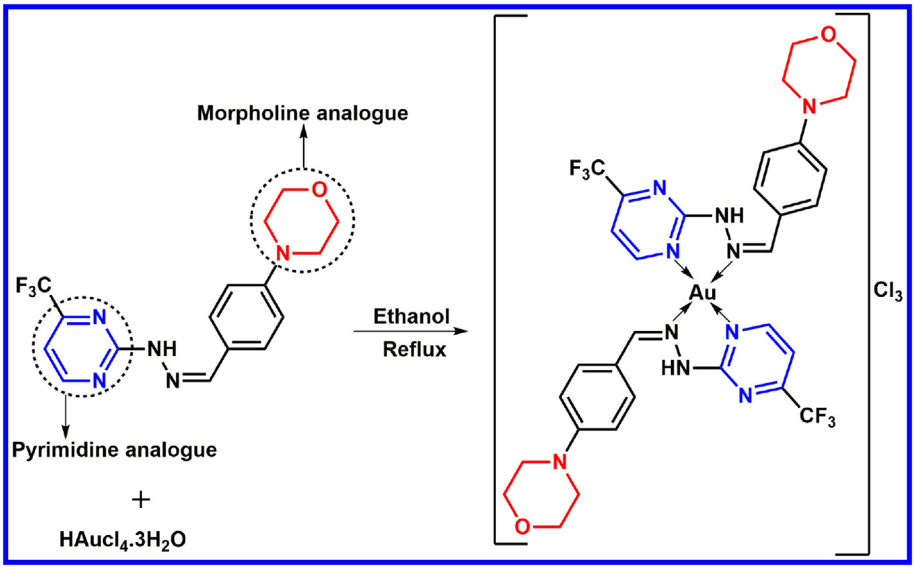

Scheme 1. Synthesis of Au(III) complex.

metal complex in tremendous conformity with the calculated values showing that Au(III) complexhas 2:1 stoichiometric ratio. The molar conductance (Λ_m) of Au(III) complexin DMSO solution was found at 73 $\Omega^{-1}cm^2mol^{-1}$ which denoted the electrolytic nature of complex.

Furthermore, formation of ligand and Au(III) complexwere confirmed by the following spectral techniques.

3.2. Spectroscopic analysis

^{1}H NMR spectra of ligand and Au(III) complexin DMSO d_6 are shown in Fig. S1 (a and b). ^{1}H NMR spectrum of free ligand, the azomethine (-CH=N-) proton signal was appeared at 8.10 ppm (s, 1H). In gold(III) complex, the –CH=N- proton signal was shifted towards downfield region at 8.67 ppm (s, 1H) indicating the azomethine nitrogen involves in the coordination of gold(III) metal ion upon complexation. Pyrimidine proton (=CH-N=) signal was appeared at 8.77 ppm (d, 1H) in free ligand. This proton signal was shifted to downfield at 8.87 ppm (d, 2H) in gold(III) complex. The result shows that pyrimidine nitrogen atom was coordinate to the gold(III) ion.

FT-IR spectra of ligand and Au(III) complexare described in Fig. S2. The FT-IR spectrum of ligand exhibit bands at 1544 cm^{-1} and 1402 cm^{-1} due to azomethine ν(-CH=N) and pyrimiding nitrogen (=CH-N=) stretching vibrations correspondingly. The spectra of Au (III) complexazomethine ν(-CH=N) and aromatic ring nitrogen (=CH-N=) stretching vibrations are observed at 1522 cm^{-1} and 1389 cm^{-1} respectively. This observation proposed that azomethine and pyrimidine nitrogen atoms are participates in the complexation.

^{1}H NMR and FT-IR spectral results suggest that gold(III) ion coordinate with azomethine and pyrimidine nitrogen atoms of Schiff base ligand.

ESI-MS spectra of ligand and Au(III) complexare shown in Fig. S3 (a and b). In ESI-MS spectum of free ligand, the molecular ion peak was observed at *m/z* 350.9. This result authenticates the formation of ligand. In gold(III) complex, the molecular ion peak at m/z, 896. These results have been suggested that stoichiometric ratio of complex possess 2:1 ratio.

Electronic absorption spectrum of free ligand, the bands detected at 266 nm and 336 nm are due to $\pi \rightarrow \pi*$ and $n \rightarrow \pi*$ transitions, correspondingly [26] (Fig. S4). This band was shifted at 270 nm and 332 nm in Au(III) complex which proves that ligand to metal charge transitions (LMCT) takes place. Au(III) complex exhibit d-d transition band at 529 nm which suggest that complex has square planar geometry.

3.3. DFT and TDDFT calculation

DFT and TDDFT calculations are used to understand the electronic structure and spectral properties of metal complexes respectively. The optimized geometry of free ligand and the metal complex is given in Fig. 1, while their highest occupied molecular orbital (HOMO) and lowest unoccupied molecular orbital (LUMO) are collected in Fig. 2. It is well known that the HOMOs and LUMOs are often used to understand not only the chemical reactivity but also stability of compounds [27,28]. The HOMO and LUMO of the ligand indicates that the flurobenzene moiety involves largely in the stabilization of LUMO while HOMO spreads throughout the molecule except tri-fluro moiety. On the other hand, the HOMO and LUMO of metal complex is very similar in nature. These results indicate that the metal complex is found to show π-π* transition along with intra-molecular charge transfer while the free ligand is expected to show intra-molecular charge transfer. The optimized geometries are used for TDDFT calculations to obtain the absorption spectra in DMSO solvent. Ploarizable continuum model (PCM) implemented in gaussian 09 has been utlized to include solvent effects in TDDFT calculations [29]. First fifty singlet vertical excitations for the metal complex and first twenty vertical excitations for free ligand have been computed along with the electronic transition energy, absorption wavelength, oscillator strength of the prominent peaks (Table S1). The results show that the metal complex shows three prominent peaks at 529 nm, 336 nm and 277 nm with the oscillator strength of 0.2197, 0.0179 and 0.0125 respectively. Peak at 529 nm resulted from the transition from HOMO→LUMO+1 which contributes up to 92% while 73% of HOMO-3 → LUMO+2 transition responsible for the peak at 336 nm. These peaks can be compared with experimentally observed peaks at 529 nm, 332 nm and 270 nm respectively. Experimental UV absorption spectrum of free ligand has two intense peaks at 266 nm and 336 nm. TDDFT calculations show that the free ligand tends to show peaks at 279 nm with excitation energy of 4.448 eV and a peak at 347 nm with oscillator strength of 0.9987. The peak at 279 nm arises due to the transition from HOMO-1 → LUMO+1 (77%) and HOMO→LUMO+1 (98%) contributes towards the peak at 347 nm.

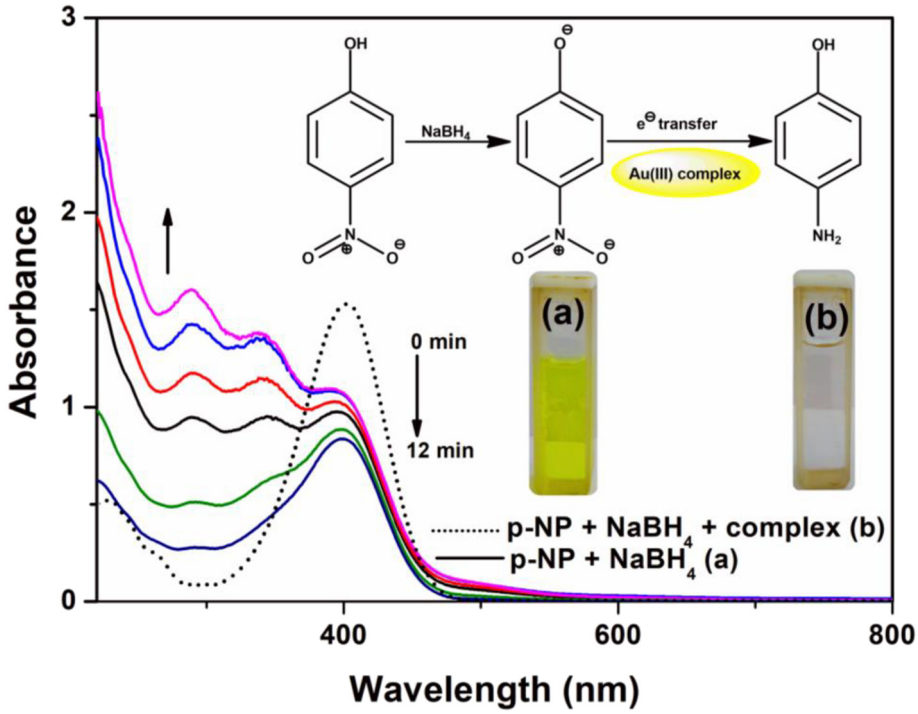

Fig. 3. Electronic absorption spectra recorded at 0–12 min showing the reduction of p-NP by $NaBH_4$ catalyzed by Au(III) complex activity.

3.4. Catalytic reduction with p-nitrophenol (p-NP)

Now, we studied the catalytic behavior of Au(III) complex for the catalytic reduction of *p*-NP to *p*-AP by using $NaBH_4$ (Fig. 3). The catalytic reduction has been examined by UV–Visible spectrophotometric method. The p-NP solution in the presence of $NaBH_4$ exhibit light yellow color to bright yellow in color and consequent band was appeared at 400 nm due to the formation p-nitrophenolate ion in alkaline medium. After the addition of Au(III) complex, the exchange of p-nitrophenolate ion into p-AP with the decrease of peak intensity at 400 nm. Concurrently, new band was appeared at 289 nm which confirms the formation of p-AP. These observed results indicates the prepared Au(III) complex have moderate catalytic activity.

3.5. Antimicrobial studies

Antimicrobial activities of ligand and Au(III) complexwere screened against bacterial (*E. coli, K. pneumonia, P. fluorescens, S. sonnei* and *S. aureus*) and fungal (*A. niger, C. albicans, C. tropicalis, M. indicus* and *Rhizopus*) species are debited in Fig. 4 (a and b). Streptomycin is standard drug for antibacterial and amphotericin is standard drug for antifungal studies. These values have been implied that Au(III) complexhas potent antimicrobial agents than ligand. Because of its molecular structure has more number of lipophilic groups. The better activity of the Au(III) complex may be assigned to the enlarged lipophilic character of these complex arising owing to the chelation and toxicity of the metal chelates increases with increasing

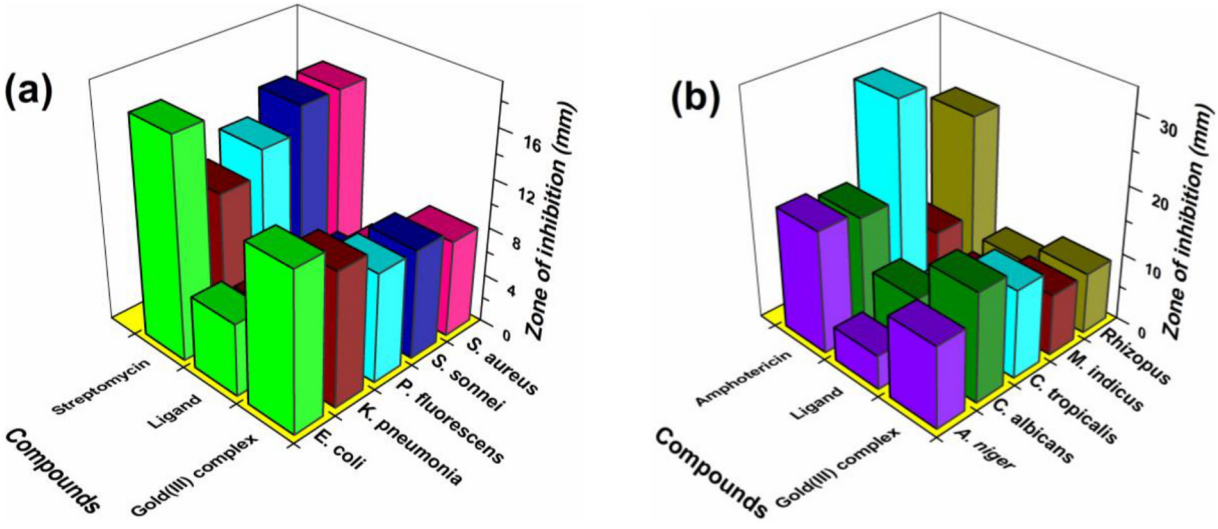

Fig. 4. Antimicrobial activities of ligand, gold(III) complex and standards Antibacterial (a) and antifungal (b).

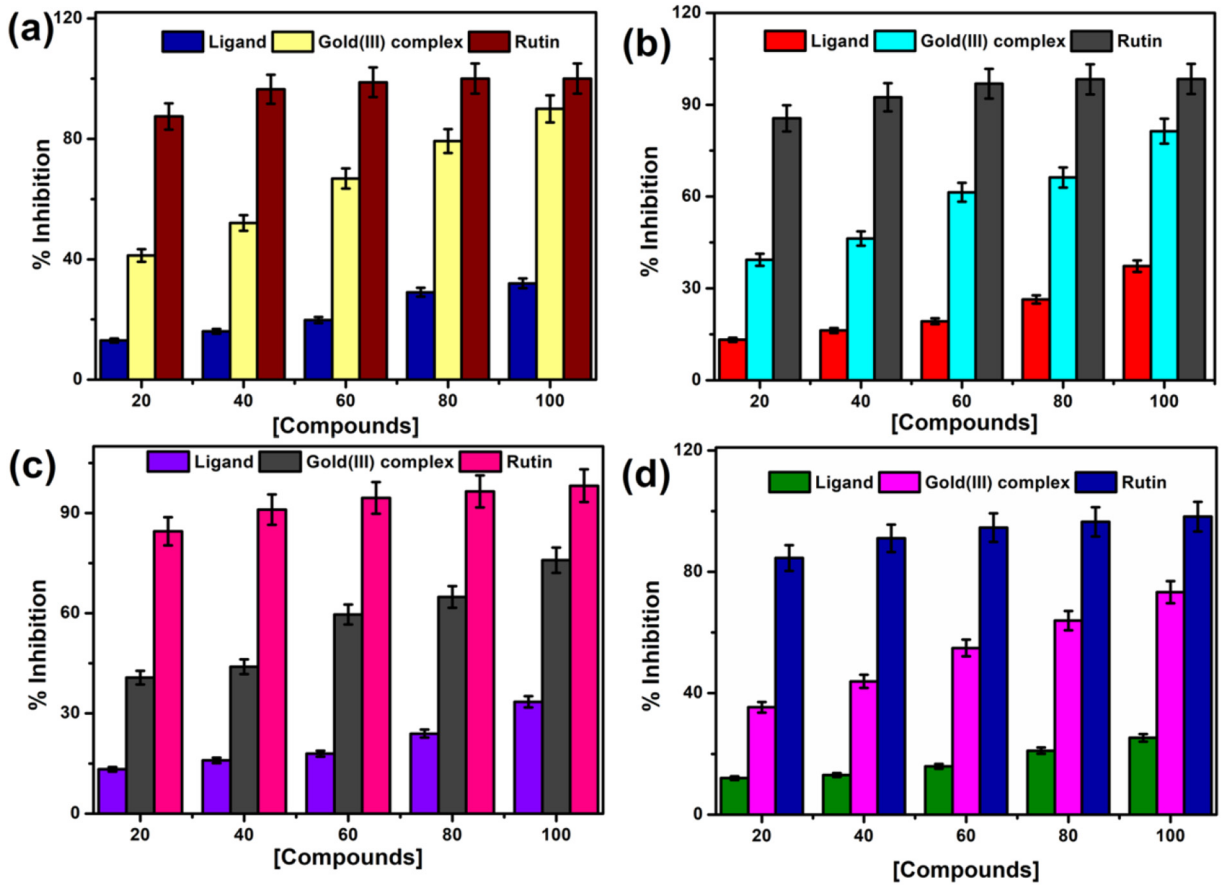

Fig. 5. Free radical scavenging activities of ligand, gold(III) complex and rutin. (a) DPPH; (b) SOD; (c) NO and (d) H_2O_2.

amount of the complex, the inhibitory activity on the mycelial growth of the microbes also raises, which can be explicated on the basis of Overtone's concept and Tweedy's Chelation theory [30]. In addition, ligand and Au(III) complexhave better inhibitory activities on *E. coli* (bacteria, 13 mm) and *C. albicans* (fungi, 16 mm) than other microbes.

3.6. Antioxidant activities

The antioxidant activities of ligand, Au(III) complexand rutin (standard drug) were examined by various free radical assays (DPPH, SOD, NO and H_2O_2). The percentage inhibitions of ligand, Au(III) complex and rutin on various free radicals are given in Fig. 5 (a-d). This results shows that the Au(III) have potent antioxidant activities against selected free radicals than ligand. The orders of radical scavenging activities are as follows: Rutin > Au(III) complex > ligand.

3.7. Anticancer studies

3.7.1. In vitro anticancer studies

In anticancer drug design and development, cytotoxicity and selectivity towards the cancer cells is one of the essential features. The *in vitro* anticancer activities of ligand, Au(III) complex and cisplatin were studied at different concentrations (20–100 μg/mL) against human cancer cell lines (MCF-7, HepG2, HeLa, A549) and single nomal cell line (NHDF) using MTT assay [31,32] (Fig. 6). MTT assay is an extensively tolerable model for the determination of the cytotoxic activity of the test compounds; hence it was selected to screen the activity. The half maximal inhibitory concentration (IC_{50}) values establish the cytotoxic activities of cisplatin, ligand and Au(III) complexagainst normal and cancer cell lines are shown in the Table 1.

(i) *Cancer cell lines*

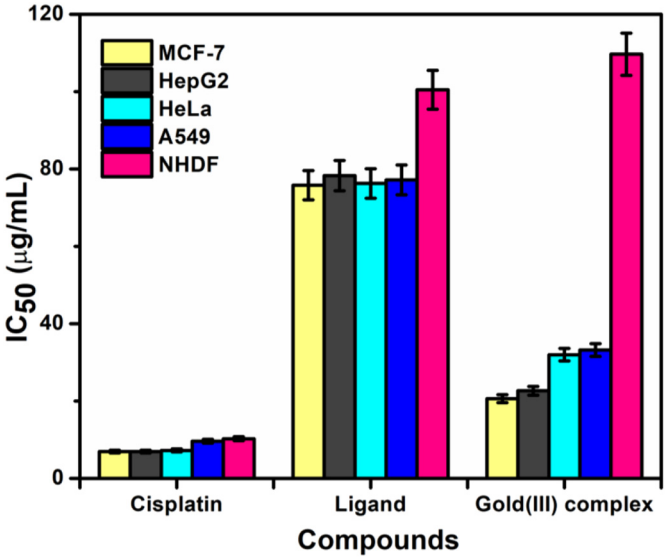

Fig. 6. *In vitro* anticancer activities of ligand and Au(III) complex.

Table 1
IC_{50} values of cisplatin, ligand and Au(III) complex towards human cancer and normal cell lines.

Compounds	IC_{50} (μg/mL)				
	MCF-7	HepG2	HeLa	A549	NHDF
Cisplatin	6.93 ± 0.35	6.94 ± 0.35	7.26 ± 0.36	9.62 ± 0.48	10.28 ± 0.51
Ligand	75.82 ± 3.79	78.25 ± 3.91	76.26 ± 3.81	77.19 ± 3.86	100.48 ± 5.02
Au(III) complex	20.6 ± 1.03	22.68 ± 1.13	32.00 ± 1.60	33.19 ± 1.66	109.65 ± 5.48

The IC_{50} values of cisplatin, ligand and Au(III) complexagainst diverse cancer cell lines in the following order: cisplatin (~6.9–7.5 μg/mL) > Au(III) complex(~20–34 μg/mL) > ligand (~75–81 μg/mL). From the order of activity, cisplatin can destroy the cancer cell lines due to the higher cytotoxic activity, but the Au(III) complexhas three times low cytotoxic effect in cancer cell lines when compared to drug cisplatin.

(ii) *Normal cell line*

The IC_{50} values of compounds against normal cell line in the following order: cisplatin (10.28 ± 0.51 μg/mL) > ligand (100.48 ± 5.02 μg/mL) > Au(III) complex (109.65 ± 5.48 μg/mL). The results reveal that, ligand and complex having 10 times least toxic activities against the normal cell line as compared to cisplatin.

(iii) *Comparative results of both cancer and normal cell lines*

As per comparison of IC_{50} values of cisplatin, ligand and Au(III) complexagainst cancer/normal cell lines results suggest that drug cisplatin can affect the both the cancer and normal cell lines. Even though, ligand having least toxic on normal cell line but did not destroy the cancer cell lines compared to gold(III) complex. But, Au(III) complex has three times low toxic and 10 times least toxic activities on cancer as well as normal cell lines as compared to cisplatin. These results established that, Au(III) complexto target the cancer cell lines without disturbing the normal cell line. These evidences are encouraged to study the *in vivo* anticancer activity of gold(III) complex.

3.7.2. Acute toxicity studies

Based on the *in vitro* results, Au(III) complex is selected for further studies. To check the acute toxicity of the Au(III) complex, Acute Oral Toxicity Studies Guideline 423 (AOT 423) was followed [19]. The results revealed that the LD_{50} cut off was found to 200 mg/kg body weight. Hence, 1/10th and 1/5th of this dose. *i.e.* 20 mg/kg and 40 mg/kg were selected for the pharmacological study.

3.7.3. In vivo anticancer activity

Mean survival time of tumor bearing mice treated with standard drug 5-flurouracil at the dose of 20 mg/kg was significantly increased when compared to tumor control group. The survival time of the treatment groups also showed significant activity when compared to tumor control group. At the same, no significant difference was observed between the groups treated with complex at 20 mg/kg and 40 mg/kg dose levels (Fig. 7). Body weight of the tumor bearing animals was found to be increased because of the accumulation of ascetic fluid and tumor burden. But the body weight was significantly reduced in the groups treated with standard and Au(III) complex which indicates the anticancer effect of the drugs (Fig. 8).

Hematological parameters of EAC tumor bearing mice on day 14 were found to be significantly altered from normal group (Table 2). There was a significant decrease in hemoglobin, RBC and lymphocytes in tumor bearing animals, accompanied by an increase in WBC, hematocrit (HCT), MID cells and protein. At the same treatment interval, complex at the dose of 20 mg/kg changed these altered parameters significantly to near normal. The dependable criteria for judging the value of any antitumor drugs are persistence of life span and decrease of WBC from blood [33]. The EAC tumor cells from the ascetic fluid of complex treated group were stained and the morphological changes were analyzed. The complex treated cells socked marked cytological changes and cytotoxic activity when compared to the cell from control group (Fig. 9). All these results suggest that the anticancer nature of the complex.

To evaluate the antitumor activity of the synthesized complex, it was subjected to study the effect on solid tumor volume produced by EAC cells. In tumor control group, the tumor volume was found to increase steadily. The groups treated with complex 1 at various dose levels

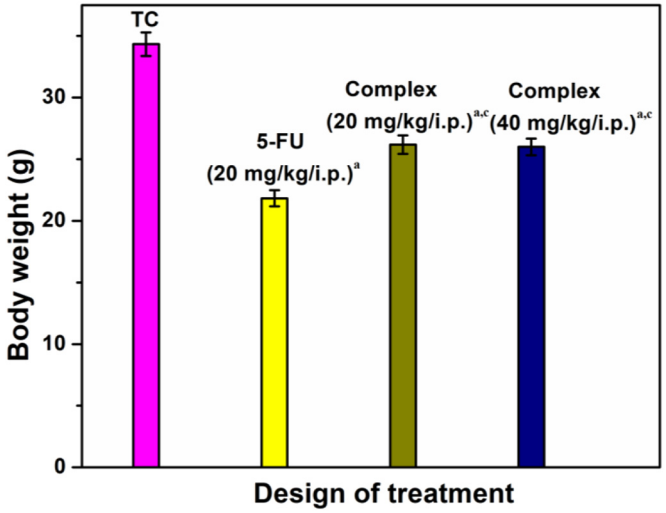

Fig. 7. Effect of Au(III) complex on body weight on EAC tumor bearing mice. TC = Tumor control, 5-FU = 5-Fluorouracil.

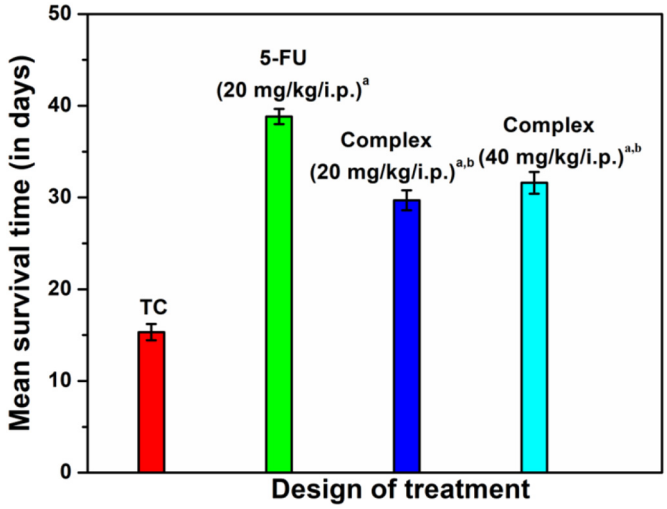

Fig. 8. Effect of Au(III) complex on survival time of EAC tumor bearing mice. TC = Tumor control, 5-Flu = 5-Fluorouracil.

Table 2
Effect of Au(III) complex on hematological parameters of EAC tumor bearing mice.

Parameters	Normal	Tumor Control	Complex 20 mg	Complex 40 mg
HGB (g/dL)	12.56 ± 0.58	6.46 ± 0.33[a]	8.98 ± 0.28[a,e]	11.74 ± 0.45[d]
RBC (M/uL)	7.16 ± 0.22	4.04 ± 0.09[a]	4.84 ± 0.32[a]	6.22 ± 0.26[d]
HCT (%)	17.66 ± 0.57	30.16 ± 1.76[a]	20.0 ± 0.79[d]	17.0 ± 0.70[d]
MCV (fL)	47.06 ± 0.82	41.8 ± 1.47[c]	45.24 ± 1.03	44.28 ± 1.17
MCH (pg)	16.72 ± 0.38	16.68 ± 0.88	17.66 ± 0.56	16.92 ± 0.95
MCHC (g/dL)	34.88 ± 0.46	37.28 ± 1.11	34.78 ± 0.51	36.22 ± 1.03
RDW (%)	17.36 ± 0.70	18.58 ± 0.44	17.76 ± 0.39	17.74 ± 0.70
PLT (K/uL)	703.2 ± 8.45	639 ± 17.33[c]	673.2 ± 15.66	713.4 ± 10.51[e]
WBC (K/uL)	4.6 ± 0.15	8.4 ± 0.40[a]	5.9 ± 0.20[b,d]	4.88 ± 1.6[d]
LYM (%)	62.38 ± 4.1	18.36 ± 1.89[a]	48.58 ± 1.36[b,d]	55.12 ± 2.45[d]
MID (%)	14.16 ± 1.61	62.72 ± 2.71[a]	24.46 ± 2.03[b,d]	21.92 ± 1.88[d]
Granulo (%)	24.3 ± 2.82	18.8 ± 2.4	26.98 ± 1.31	22.96 ± 3.69
Total Proteins (g/dL)	5.35 ± 0.11	14.27 ± 0.42[a]	10.2 ± 0.36[a,d]	9.28 ± 0.27[e]

$N = 10$; Data were expressed as Mean ± SEM. Data were analyzed by One way ANOVA followed by Tukey Kramer Multiple comparison test.
[a] $P < 0.001$.
[b] $P < 0.01$.
[c] $P < 0.05$ *vs* Normal.
[d] $P < 0.001$.
[e] $P < 0.01$ *vs* Tumor Control.

significantly reduce the solid tumor volume which indicates the cytotoxic nature of the synthesized complex. There is no significant difference was observed between the tested dose levels (Fig. 10).

In vivo studies results suggest that our synthesized complex is having potential anticancer activities. Therefore, additional investigation is needed in order to discover the prospective of the complex in cancer treatment may prove to be valuable.

3.8. DNA interaction studies

3.8.1. Absorption spectral titration

The UV–Visible spectra of ligand and Au(III) complex in the presence and absence of CT-DNA were appraised by absorption spectral titrations are presented in Fig. 11. As exposed in Fig. 10, the concentration of CT-DNA increases to a solution of ligand and Au(III) complexlead to hypochromism (6.27%, ligand and 17.19%, Au(III) complex) with a slight red shifts (3 and 4 nm). This result obviously indicated that compounds can interact with CT-DNA *via* intercalative interaction due to the presence of pyrimidine and morpholine analogues. In order to discover the intrinsic binding constants (K_b) of ligand and Au(III) complex by using the following Eq. [20],

$$[DNA]/\varepsilon_a - \varepsilon_f = [DNA]/\varepsilon_b - \varepsilon_f + \left[K_b\left(\varepsilon_b - \varepsilon_f\right)\right]^{-1}$$

The K_b values of ligand and Au(III) complexare $2.65 \times 10^3\ M^{-1}$ and $4.97 \times 10^4\ M^{-1}$) are shown in Table 3. The obtained K_b values of compounds are small as compared to ethidium bromide (EB = $1.4 \times 10^6\ M^{-1}$). The lower K_b values for compounds are due to the presence of flexible versatile morpholine analogue in its structural framework which significantly facilitates intercalation with the base pairs.

3.8.2. Competitive interaction with DNA

Furthermore, in order to verify the interaction of ligand and Au(III) complex with CT-DNA, displacement assay was carried out using ethidium bromide (EB). The EB bound DNA was titrated with the increasing concentrations of ligand and gold(III) complex, decrement of emission intensity as shown in Fig. 12 The binding tendency of the ligand and Au(III) complex to EB bound DNA were measured by Stern-Volmer equation using the following equation [21],

$$F_0/F = 1 + Kq\tau_0[Q] = 1 + K_{SV}\,[Q]$$

Moreover, binding affinity (K_{app}) of ligand and Au(III) complexin comparison of ethidium bromide was calculated by using the following equation,

$$K_{EB}\,[EB] = K_{app}\,[Complex]$$

The calculated K_{SV}, $K_q$and K_{app} values suggest that Au(III) complex have higher binding activity than ligand. The absorption titration results were correlated with displacement results suggest that ligand and Au (III) complex bind to DNA *via* strong intercalation. The binding constant

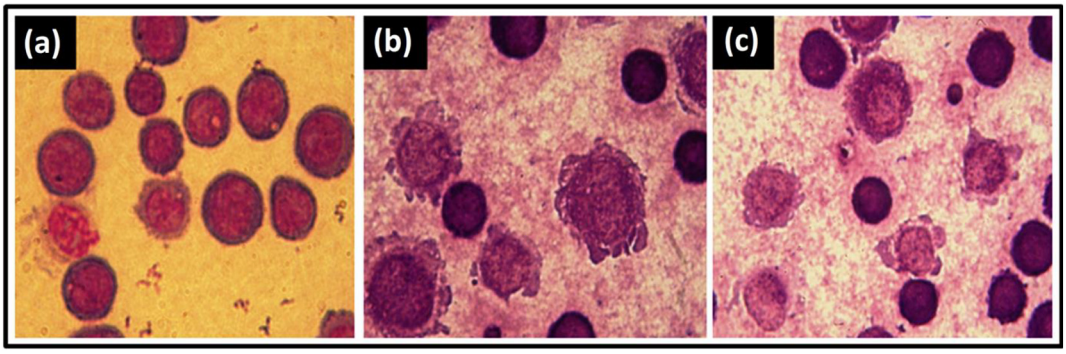

Fig. 9. (a) Smear showing matured EAC cells with definite structure and clear cell wall without degeneration, (b) EAC tumor cells treated with Au(III) complex showing degenerative changes in the form of membrane blebbing and disintegration, (c) EAC cells treated with Au(III) complex showing degenerative changes like membrane bleebing, cell wall destruction, cell disintegration and a reduction in staining intensity.

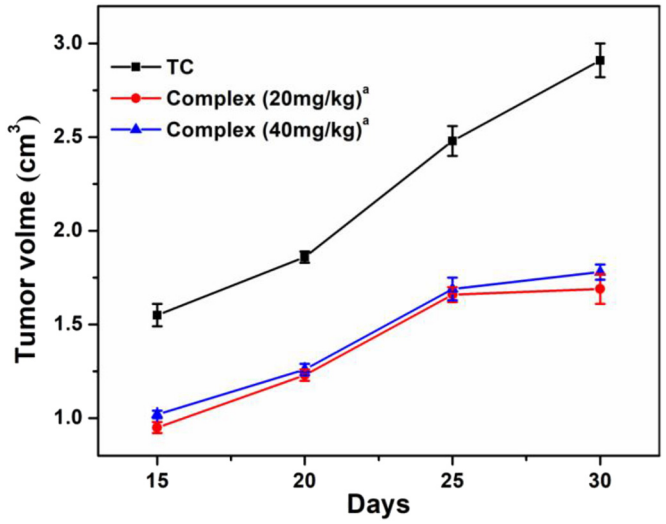

Fig. 10. Effect of Au(III) complex on tumor volume of EAC tumor bearing mice. TC = Tumor control, 5-FU = 5-Fluorouracil.

(K_a) and binding sites (n) of ligand and Au(III) complex were calculated by following equation. The values of K_a and n are shown in Table 4.

$$log\frac{F_0 - F}{F} = \log K_a + n \log[Q]$$

The calculated n value of ligand and Au(III) complexare near to unity. This shows that compounds bound with DNA *via* single class site.

3.8.3. Electrochemical studies

As further exploring the binding of the Au(III) complex with CT-DNA, cyclic voltammetric studies were carried out both in the presence and absence of CT-DNA. A typical CV behavior of complex in the presence and absence of excess DNA is shown in Fig. 13. When the addition of DNA to the complex results peak current intensity increases and potential shifted towards negative direction. From this examination, complex bind with DNA through intercalative mode is confirmed.

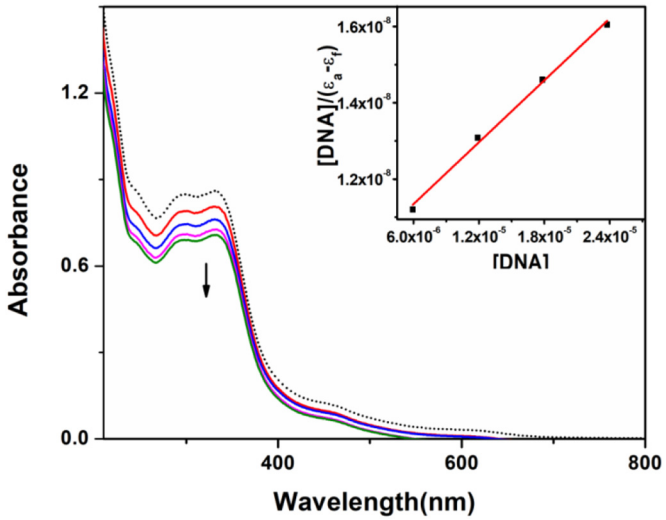

Fig. 11. Absorption spectral titration of Au(III) complex in the presence and absence of CT-DNA in Tris-HCl buffer at pH 7.0.

Table 3
Absorption spectral properties of ligand and Au(III) complex on binding to CT-DNA.

Compounds	λ_{max} (nm)		Δλ (nm)	Hypochromism (%)	K_b (M^{-1})
	Free	Bound			
Ligand	336	339	3.0	6.27	2.65×10^3
Au(III) complex	332	336	4.0	17.19	4.97×10^4

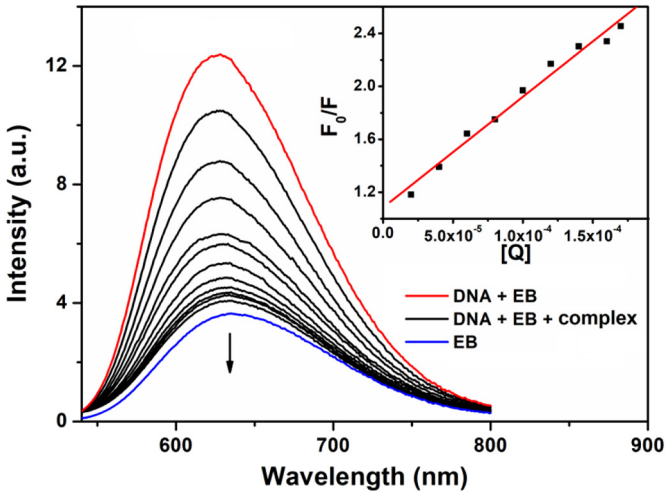

Fig. 12. Fluorescence spectra of Au(III) complex with EB bound DNA.

3.8.4. Viscometric measurements

The viscometric measurements are helpful to elucidate the binding nature of ligand and gold(III) complex. The graph of relative viscosity *vs* [compounds] / [DNA] were described in Fig. 14 As a result the concentrations of ligand and Au(III) complexincreases and the viscous flow of DNA increases. These observations have been indicated that interaction can be done between compounds and CT-DNA.

3.9. Molecular modeling with DNA / BSA

In order to identify the binding affinity of the Au(III) complex and the free ligand towards DNA and BSA protein, a detailed molecular docking analysis is carried out using Autodock Vina software. The most favorable binding mode for the gold and free ligand towards DNA and BSA protein are given in Fig. 15 (a and b) and Fig. 16 (a and b). From the molecular docking calculations, it is clear that the gold complex binds to the DNA double helix in an intercalation fashion with the binding energy of 9.3 kcal/mol. The free ligand shows relatively poor binding ability towards DNA with 6.7 kcal/mol. It is interesting to note that similar trend is observed in the BSA binding studies. The ligand molecule shows 9.3 kcal/mol binding energy while 11.1 kcal/mol binding energy is obtained for gold complex towards BSA protein. The active site residues of ligand bound BSA protein are Try 149, Tyr 156, Arg 198, His 241, Arg 256 Leu 259, Ala 260, Ser 286 and Ala 290 respectively. It is important to note that the ligand is showing three hydrogen bonds with Try 149, His 241 and Arg 256 residues. Gold complex shows a hydrogen bond with His 145 and the other active site residues are Arg 185, Leu

Table 4
Binding parameters of the ligand and Au(III) complex with EB bound DNA.

Compounds	K_{sv} ($L\,mol^{-1}$)	K_q ($L\,mol^{-1}\,s^{-1}$)	K_{app} ($L\,mol^{-1}$)	K_a ($L\,mol^{-1}$)	n
Ligand	3.30×10^3	3.30×10^{11}	2.15×10^5	4.09×10^5	1.08
Gold(III) complex	8.37×10^3	8.37×10^{11}	5.30×10^6	3.98×10^5	1.04

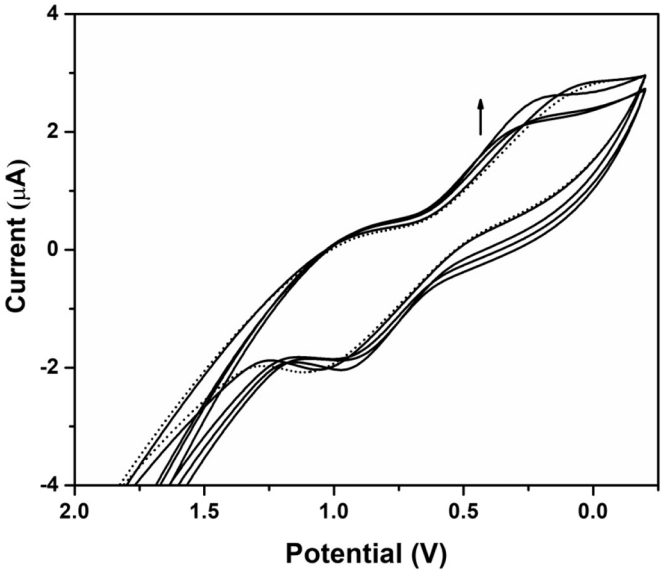

Fig. 13. Electrochemical studies of Au(III) complex in the presence and absence of CT-DNA at 100 mV.

189, Thr 190, Ser 192, Pro 240, Glu 424, Ser 428, Ile 522 and Arg 458. Both the metal complex and the free ligand is stabilized by other non-covalent interactions and the binding energy trend is in total agreement with the experiments.

4. Conclusion

In summary, we have synthesized Au(III) complex from pyrimidine and morpholine analogues of Schiff base ligand. The elemental and mass spectrometric data of Au(III) complex confirms the stoichiometry ratio is 2:1 ratio (ML_2 type). It has structurally characterized by various spectral techniques and results have been suggested that, Au(III) complex adopt square planar geometry around the central metal atom. Antimicrobial and antioxidant activities results suggest that, Au(III) complex has better antimicrobial and radical scavenging activities. *In vitro* anticancer activity of ligand and Au(III) complex were analyzed by MTT assay. Interestingly, Au(III) complex is destroyed the cancer cell lines but least toxic against normal cell line in contrast to cisplatin. These observation shows that, Au(III) complex is ten times least toxic effect normal cell line than others which is obtained from gold metal based Schiff base ligand containing pyrimidine and morpholine linkage.

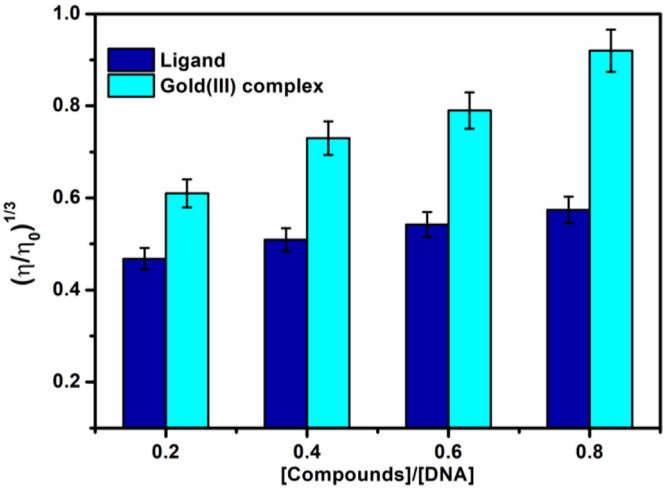

Fig. 14. Effective relative viscosity of increasing concentrations of CT-DNA to the ligand and Au(III) complex.

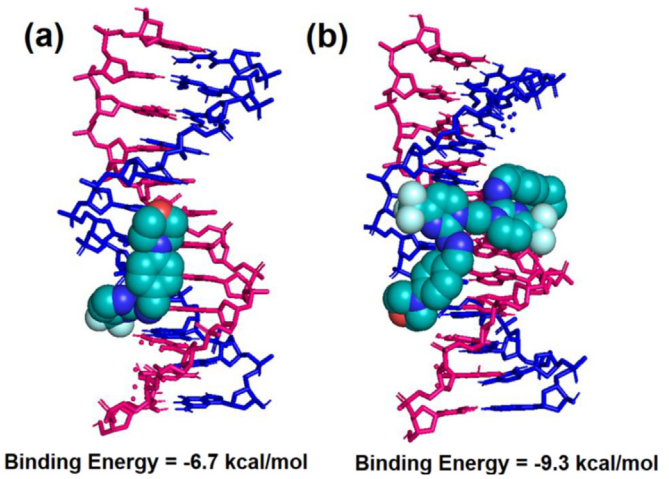

Fig. 15. The best possible binding pose of the free ligand (a) and Au(III) complex (b) into the DNA double helix from our molecular docking analysis (ligand and Au(III) complex are given in space filling model).

Furthermore, *in vivo* studies of synthesized Au(III) complex on tumor bearing mice results show that the Au(III) complex have potential anticancer ability. TDDFT calculations substantiate the experimentally observed absorption spectra of both metal complex and free ligand while molecular docking studies offer insights into the binding affinities of metal complex and free ligand towards DNA and BSA protein. Molecular docking results indicate that the binding ability gold complex is greater than that of the free ligand. Both the complex and the free ligand are stabilized by hydrogen bonding interactions along with other weak non-

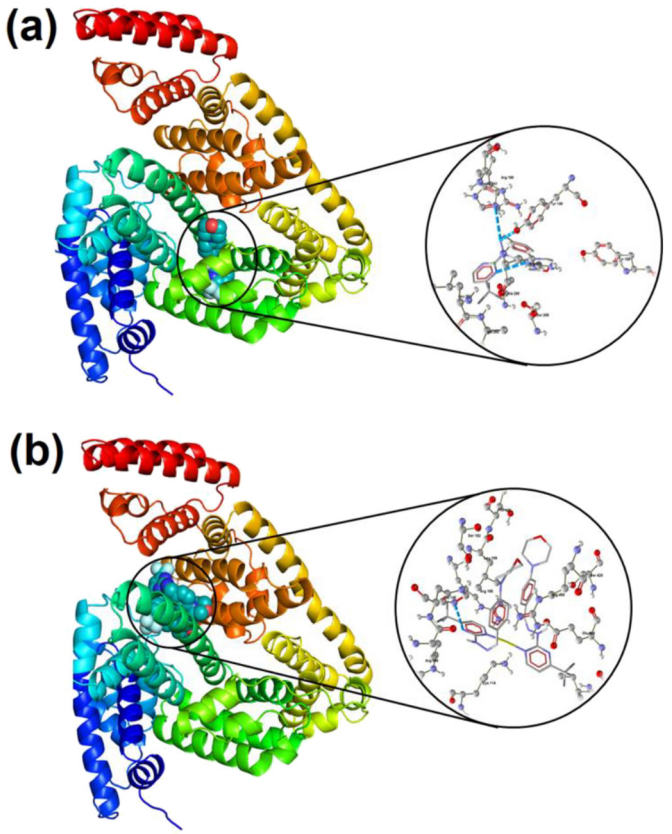

Fig. 16. The best possible binding pose of the free ligand (a) and Au(III) metal complex (b) into the BSA from our molecular docking analysis. (Hydrogen atoms are omitted for clarity and hydrogen bonding is indicated by dotted line.)

covalent interactions. The DNA interaction results show that, ligand and Au(III) complex bind with DNA *via* intercalative mode of binding. Further studies are needed to prove the chemotherapeutic properties of gold complex based Schiff base ligand bearing pyrimidine and morpholine substituents.

Acknowledgements

The authors acknowledge the Department of Science and Technology (DST)-Science and Engineering Research Board (SERB Ref. No.: SR/FT/CS-117/2011 dated 29.06.2012), Government of India, New Delhi for the financial support.

Appendix A. Supplementary data

Supplementary data to this article can be found online at https://doi.org/10.1016/j.molliq.2019.111655.

References

[1] S. Rafique, M. Idrees, A. Nasim, H. Akbar, A. Athar, Transition metal complexes as potential therapeutic agents, Biotechnol. Mol. Biol. Rev. 5 (2010) 38–45http://www.academicjournals.org/BMBR.
[2] Y. Jung, S.J. Lippard, Direct cellular responses to platinum-induced DNA damage, Chem. Rev. 107 (2007) 1387–1407, https://doi.org/10.1021/cr068207 j.
[3] M.H. Gracia, T.S. Morais, P. Florindo, M.F.M. Piedade, V. Moreno, C. Ciudad, V. Noe, Inhibition of cancer cell growth by ruthenium(II) cyclopentadienyl derivative complexes with heteroaromatic ligands, J. Inorg. Biochem. 103 (2009) 354–361, https://doi.org/10.1016/j.jinorgbio.2008.11.016.
[4] C.H. Wu, D.H. Wu, X. Liu, G. Guoyiqibayi, D.D. Guo, G. Lv, X.M. wang, H. Yan, H. Jiang, Z.H. Lu, Ligand-based neutral ruthenium(II) arene complex: selective anticancer action, Inorg. Chem. 48 (2009) 2352–2354. doi:https://doi.org/10.1021/ic900009j.
[5] E. Kim, P.T. Rye, J.M. Essigmann, R.G. Croy, A bifunctional platinum(II) antitumor agent that forms DNA adducts with affinity for the estrogen receptor, J. Inorg. Biochem. 103 (2009) 256–261, https://doi.org/10.1016/j.jinorgbio.2008.10.013.
[6] M.N. Patel, B.S. Bhatt, P.A. Dosi, DNA binding, cytotoxicity and DNA cleavage promoted by gold(III) complexes, Inorg. Chem. Commun. 29 (2013) 190–193, https://doi.org/10.1016/j.inoche.2012.12.013.
[7] L. Ronconi, L. Giovagnini, C. Marzano, F. Bettio, R. Graziani, G. Pilloni, D. Fregona, Gold dithiocarbamate derivatives as potential antineoplastic agents: design, spectroscopic properties, and in vitro antitumor activity, Inorg. Chem. 44 (2005) 1867–1881, https://doi.org/10.1021/ic048260v.
[8] S. Sangeetha, M. Murali, Water soluble copper(II) complex [cu(dipica)(CH_3COO)]ClO_4: DNA binding, pH dependent DNA cleavage and cytotoxicity, Inorg. Chem. Commun. 59 (2015) 46–49, https://doi.org/10.1016/j.inoche.2015.06.032.
[9] K. Nagaraj, K.S. Murugan, P. Thangamuniyandic, S. Sakthinathan, Nucleic acid binding study of surfactant copper(II) complex containing dipyrido [3,2-a:2′-3′-c]phenazine ligand as an intercalator: in vitro antitumor activity of complex in human liver carcinoma (HepG2) cancer cells, RSC Adv. 4 (2014) 56084–56094, https://doi.org/10.1039/c4ra08049a.
[10] N. Shahabadi, M. Hakimi, T. Morovati, M. Falsai, S.M. Fili, Experimental and molecular modeling studies on the DNA-binding of diazacyclam-based arocyclic copper complex, J. Photochem. Photobiol. B 167 (2017) 7–14, https://doi.org/10.1016/j.jphotobiol.2016.12.023.
[11] S.R. Grguric-Sipka, R.A. Vilaplana, J.M. Perez, M.A. Fuertes, C. Alonso, Y. Alvarez, T.J. Sabo, F. Gonzalez-Vilchez, Synthesis, characterization, interaction with DNA and cytotoxicity of the new potential antitumour drug cis-K[Ru(eddp)Cl_2], J. Inorg. Biochem. 97 (2003) 215–220, https://doi.org/10.1016/s0162-0134(03)00281-2.
[12] S. Rauf, J.J. Gooding, K. Akhtar, M.A. Ghauri, M. Rahman, M.A. Anwar, A.M. Khalid, Electrochemical approach of anticancer drugs–DNA interaction, J. Pharm. Biomed. Anal. 37 (2005) 205–217, https://doi.org/10.1016/j.jpba.2004.10.037.
[13] S.N. Podyachev, V.E. Semenov, V.V. Syakaev, N.E. Kashapova, S.N. Sudakova, J.K. Voronina, A.S. Mikhailov, A.D. Voloshina, V.S. Reznik, A.I. Konovalov, Metal binding properties of pyrimidinophanes and their acyclic counterparts, RSC Adv. 4 (2014) 10228–10239, https://doi.org/10.1039/c3ra47571a.
[14] M. Sankarganesh, J. Rajesh, G.G. Vinoth Kumar, M. Vadivel, L. Mitu, R. Senthil Kumar, J. Dhaveethu Raja, Synthesis, spectral characterization, theoretical, antimicrobial, DNA interaction and in vitro anticancer studies of Cu(II) and Zn(II) complexes with pyrmidine-morpholine based Schiff base ligand, J. Saudi Chem. Soc. 22 (2018) 416–426, https://doi.org/10.1016/j.jscs.2017.08.007.
[15] J. Lakshmipraba, S. Arunachalam, R.V. Solomon, P. Venuvanalingam, A. Riyasdeen, R. Dhivya, M.A. Akbarsha, Surfactant–copper(II) Schiff base complexes: synthesis, structural investigation, DNA interaction, docking studies, and cytotoxic activity, J. Biomol. Struct. Dyn. 38 (2015) 877–891, https://doi.org/10.1080/07391102.2014.918523.
[16] J. Lakshmipraba, S. Arunachalam, R. Vijay Solomon, P. Venuvanalingam, Synthesis, DNA binding and docking studies of copper(II) complexes containing modified phenanthroline ligands, J. Coord. Chem. 68 (2015) 1374, https://doi.org/10.1080/00958972.2015.1014349.
[17] M. Sankarganesh, N. Revathi, J. Dhaveethu Raja, K. Sakthikumar, G.G. Vinoth Kumar, J. Rajesh, M. Rajalakshmi, L. Mitu, Computational, antimicrobial, DNA binding and anticancer activities of pyrimidine incorporated ligand and its copper(II) and zinc (II) complexes, J. Serb. Chem. Soc. 83 (2019) 277–291, https://doi.org/10.2298/jsc180609080s.
[18] W. Liu, J. Jiang, Y. Xu, S. Hou, L. Sun, Q. Ye, L. Lou, Design, synthesis and anticancer activity of diam(m)ine platinum(II) complexes bearing a small-molecular cel apoptosis inducer dichloroacetate, J. Inorg. Biochem. 146 (2015) 14–18, https://doi.org/10.1016/j.jinorgbio.2015.02.002.
[19] R. Senthil Kumar, B. Rajkapoor, P. Perumal, In vitro and in vivo anticancer activity of Indigofera cassioides Rottl. Ex. DC, Asian Pac. J. Trop. Med.4 (2011) 379–385. doi: https://doi.org/10.1016/s1995-7645(11)60108-9.
[20] M. Sankarganesh, J. Dhaveethu Raja, K. Sakthikumar, R. Vijay Soloman, J. Rajesh, S. Athimoolam, V. Vijayakumar, New bio-sensitive and biologically active single crystal of pyrimidine scaffold ligand and its gold and platinum complexes: DFT, antimicrobial, antioxidant, DNA interaction, molecular docking with DNA / BSA and anticancer studies, Bioorg. Chem. 81 (2018) 144–156, https://doi.org/10.1016/j.bioorg.2018.08.006.
[21] M. Sankarganesh, J. Dhaveethu Raja, P. Adwin Jose, G.G. Vinoth Kumar, J. Rajesh, R. Rajasekaran, Spectroscopic, computational, antimicrobial, DNA interaction, in vitro anticancer and molecular docking properties of biochemically active cu(II) and Zn (II) complexes of pyrimidine-ligand, J. Fluoresc. 28 (2018) 975–985, https://doi.org/10.1007/s10895-018-2261-0.
[22] M. Frisch, G. Trucks, H. Schlegel, G. Scuseria, M. Robb, J. Cheeseman, G. Scalmani, V. Barone, B. Mennucci, G. Petersson, H. Nakatsuji, M. Caricato, X. Li, H. Hratchian, A. Izmaylov, J. Bloino, G. Zheng, J. Sonnenberg, M. Hada, M. Ehara, K. Toyota, R. Fukuda, J. Hasegawa, M. Ishida, T. Nakajima, Y. Honda, O. Kitao, H. Nakai, T. Vreven, J.J. Montgomery, J. Peralta, F. Ogliaro, M. Bearpark, J. Heyd, E. Brothers, K.N. Kudin, V. Staroverov, R. Kobayashi, J. Normand, K. Raghavachari, A. Rendell, J. Burant, S. Iyengar, J. Tomasi, M. Cossi, N. Rega, N. Millam, M. Klene, J. Knox, J. Cross, V. Bakken, C. Adamo, J. Jaramillo, R. Gomperts, R. Stratmann, O. Yazyev, A. Austin, R. Cammi, C. Pomelli, J. Ochterski, R.L. Martin, K. Morokuma, V. Zakrzewski, G. Voth, P. Salvador, J. Dannenberg, S. Dapprich, A. Daniels, O. Farkas, J. Foresman, J. Ortiz, J. Cioslowski, D. Fox, Gaussian 09, R. B., Gaussian, Inc., Wallingford CT, 2009.
[23] O. Trott, A.J. Olson, AutoDock Vina: improving the speed and accuracy of docking with a new scoring function, efficient optimization, and multithreading, J. Comput. Chem. 31 (2010) 455, https://doi.org/10.1002/jcc.v31:1.
[24] A. Bujacz, Acta Crystallogr. D Biol. Crystallogr. 68 (2012) 1278, https://doi.org/10.1107/s0907444912027047.
[25] I. Ullah, K. Khan, M. Sohail, K. Ullah, A. Ullah, S. Shaheen, Synthesis, structural characterization and catalutic applications of citrate-stabilized monometallic and bimetallic palladium@copper nanoparticles in microbial anti-activities, Int. J. Nanomedicine 12 (2017) 8735–8747, https://doi.org/10.2147/IJN.S145085.
[26] A.B.P. Lever, Inorganic Electronic Spectroscopy, Amsterdam, 1984.
[27] R.V. Solomon, P. Veerapandian, S.A. Vedha, P. Venuvanalingam, Tuning nonlinear optical and optoelectronic properties of vinyl coupled Triazene chromophores: a density functional theory and time-dependent density functional theory investigation, J. Phys. Chem. A 116 (2012) 4667, https://doi.org/10.1021/jp302276w.
[28] R.V. Solomon, R. Jagadeesan, S.A. Vedha, P. Venuvanalingam, A DFT/TDDFT modelling of bithiophene azo chromophores for optoelectronic applications, Dyes Pigments 100 (2014) 261, https://doi.org/10.1016/j.dyepig.2013.09.016.
[29] M. Cossi, V. Barone, R. Cammi, J. Tomasi, Ab initio study of solvated molecules: a new implementation of the polarizable continuum model, Chem. Phys. Lett. 255 (1996) 327, https://doi.org/10.1016/0009-2614(96)00349-1.
[30] L.F. Larkworthy, M.W.O. Donoghue, Synthesis and properties of vanadium(III) dithiocarbamates, Inorg. Chim. Acta 74 (1983) 155–158, https://doi.org/10.1016/s0020-1693(00)81422-x.
[31] N. Pravin, G. Kumaravel, R. Senthil Kumar, N. Raman, Water-soluble Schiff base Cu (II) and Zn(II) complexes: synthesis, DNA targeting ability and chemotherapeutic potential of cu(II) complex for hepatocellular carcinoma in vitro and in vivo approach, Appl. Organometal. Chem. (2017), e3739. https://doi.org/10.1002/aoc.3739.
[32] N. Revathi, M. Sankarganesh, J. Rajesh, J. Dhaveethu Raja, Biologically active cu(II), co(II), Ni(II) and Zn(II) complexes of pyrimidine derivative Schiff base: DNA binding, antioxidant, antibacterial and in vitro anticancer studies, J. Fluoresc. 27 (2017) 1801–1814, https://doi.org/10.1007/s10895-017-2118-y.
[33] C. Oberling, M. Guerin, The role of viruses in the production of cancer, Adv. Cancer Res. 2 (1954) 353–423, https://doi.org/10.1016/s0065-230x(08)60499-6.